

Sensor fault diagnosis technique applied to three-phase induction motor drive

Tien Xuan Nguyen¹, Minh Chau Huu Nguyen^{2,3}, Cuong Dinh Tran⁴

¹Faculty of Electronics and Telecommunication, Saigon University, Vietnam

²Faculty of Electrical Engineering and Computer Science, VSB-Technical University of Ostrava, Czech Republic

³Faculty of Electrical and Electronics Engineering, Vietnam Aviation Academy, Vietnam

⁴Power System Optimization Research Group, Faculty of Electrical and Electronics Engineering, Ton Duc Thang University, Ho Chi Minh City, Vietnam

Article Info

Article history:

Received Jun 15, 2022

Revised Jul 25, 2022

Accepted Aug 19, 2022

Keywords:

Diagnosis method
Fault detection
Fault-tolerant control
Induction motor
Sensorless

ABSTRACT

This paper conducts research on sensor fault diagnosis for a three-phase induction motor drive (IMD) in steady-state operation. An improving diagnostic technique based on the integration algorithm of the sinusoidal current signal is proposed for detecting and locating faulty current sensors in the induction motor drive. The IMD integrated a proposed fault detection-isolation (FDI) system is investigated for operating characteristics when sensor failures occur. The faulty sensor needs to be accurately identified and quickly isolated from the control system. Then the estimated signal will be used to replace the fault signal to retain the IMD stability. MATLAB/Simulink software will be applied to simulate the speed-torque characteristics of the IMD system as well as sensor failures occurring during operation. The performance of the proposed method will be evaluated through the accuracy and timeliness in each fault case corresponding to each sensor.

This is an open access article under the [CC BY-SA](https://creativecommons.org/licenses/by-sa/4.0/) license.



Corresponding Author:

Cuong Dinh Tran

Power System Optimization Research Group, Faculty of Electrical and Electronics Engineering

Ton Duc Thang University

19 Nguyen Huu Tho, District 7, Ho Chi Minh City, Vietnam

Email: trandinhuong@tdtu.edu.vn

1. INTRODUCTION

By the end of the 18th century, induction motors (IMs) had become the most popular electrical machine in the industry, with outstanding advantages over direct current (DC) motors such as ruggedness, low rotor inertia, small size, and low cost [1], [2]. However, speed controlling of IMs is still challenging due to the nonlinear control characteristic. By applying mathematical models such as expert-system, fuzzy logic, neural-network control, and genetic algorithm, the induction motor drive (IMD) could be used to control the speed for industrial applications with high efficiency.

The vector control method, typically the field-oriented control (FOC) method, has emerged as a highly effective solution in the field of electric machine speed control [3]–[5]. The feedback signals of the sensors that provide the instantaneous operating state of the drive play a crucial role in the motor control system [6]. Therefore, if there is any damage to the sensor, which leads to an inaccurate reflection of the motor's operating state, the reliability of the vector control method will be degraded and may cause damage to equipment or economic loss [7], [8]. Many control methods integrating the fault sensor diagnosis technique have been focused on research to increase the stability, reliability, and continuity of the IMDs in recent years [9], [10]. Stator current and the rotor speed signals are the two most crucial feedback signal

types that determine the performance of the FOC method. If a feedback failure occurs, the FOC control algorithm can make a mistake, leading to an incorrect switching signal supplied to the inverter. In various approaches, sensor fault diagnosis algorithms may be implemented for analyzing the two types of current and speed failures separately or with mutual influence. In research corresponding to the speed fault diagnosis techniques, most algorithms are based on the similarity analysis of the estimated signal and the feedback signal from the encoder. In [11]–[13], the deviation between the measured rotor speed and the estimated signals from filters such as Kalman, flux observer, and Luenberger observer when exceeds one predefined threshold are applied for speed sensor fault detection.

Various methods of fault detection of current faults have been developed depending on the number of current sensors used in the drive system and the type of fault diagnosis technique. Fault diagnosis techniques in IMD using three current sensors are often built based on Kirchoff's law of current [14]. Three current-state observers are designed based on the respective two-phase currents. The output difference between these observers is the main factor in identifying the fault current sensor [15], [16]. However, in IMD designed to use only two current sensors, Kirchoff's law cannot be applied to the location of the faulty sensor. Current sensor fault diagnosis methods using only two sensors in IMD are classified into main groups: i) the algorithms are based on a comparison of the measured and the estimated signals to determine the faulty sensor [17], [18], ii) the algorithms are based on verifying the abnormal change of each measured signal to evaluate the quality of the feedback signals [7], [19], iii) the algorithms for verifying the stability of a complex combination function to detect the abnormal state of the measured signals [20], and iv) algorithms combining the above methods.

This paper aims to propose a diagnosis method based on the combination of the feedback signal, its integration algorithm to determine the fault state of the feedback current signal, a typical comparison algorithm between the measured signal, and the estimated signal of the rotor speed is applied to determine the operating status of the speed encoder. If the feedback signal is incorrect due to sensor failure, the signal is immediately isolated and replaced with the appropriate estimated signals [21]–[28]. The diagnosis results are used to evaluate the performance of the proposed methods with various sensor faults in the MATLAB/Simulink environment.

2. METHOD: SENSOR FAULT DIAGNOSIS TECHNIQUE

The state variable equations of the three-phase induction motor and the proposed sensor fault diagnosis algorithm are presented in this section.

2.1. The state variable equations of the three-phase IM

The nonlinear characteristic of a three-phase IM is described in the form of state variable equations in the stationary frame $[\alpha\text{-}\beta]$ as (1):

$$\dot{X} = M \cdot X + I \cdot U \quad (1)$$

Where:

$$X = [i_{S\alpha} i_{S\beta} \psi_{R\alpha} \psi_{R\beta}]^T; U = [u_{S\alpha} u_{S\beta}]; M = \begin{bmatrix} -A & B & C & \omega_r \\ 0 & -A & -C & \omega_r \\ E & 0 & -F & -\omega_r \\ 0 & E & \omega_r & -F \end{bmatrix}; I = \begin{bmatrix} D & 0 & 0 & 0 \\ 0 & D & 0 & 0 \end{bmatrix}^T$$

$$A = \frac{R_s L_r^2 + R_r L_m^2}{\sigma L_s L_r^2}; B = \frac{R_r L_m}{\sigma L_s L_r^2}; C = \frac{L_m}{\sigma L_s L_r}; D = \frac{1}{\sigma L_s}; E = \frac{R_r L_m}{L_r}; F = \frac{R_r}{L_r}; \sigma = \frac{L_s L_r - L_m^2}{L_s L_r}$$

Where: “ $\omega_r = p\omega_m$ ”: the value of the rotor speed

“p”: number of pole pairs

“ ω_m ”: mechanical rotor speed

In this research, the FOC loop corresponding to the block diagram in Figure 1 is used in precise speed-torque control for the IMD. Clark-Park's formulas are applied to transform feedback currents to the components in stationary $[\alpha\text{-}\beta]$ and rotating $[x\text{-}y]$ systems. The mathematical formulas describing the method of transformation and estimating signals for the control are shown:

$$\begin{bmatrix} i_{S\alpha} \\ i_{S\beta} \end{bmatrix} = \begin{bmatrix} 1 & 0 \\ \frac{1}{\sqrt{3}} & \frac{2}{\sqrt{3}} \end{bmatrix} \begin{bmatrix} i_a \\ i_b \end{bmatrix} \quad (2)$$

$$\begin{bmatrix} i_{sx} \\ i_{sy} \end{bmatrix} = \begin{bmatrix} \cos \gamma & \sin \gamma \\ -\sin \gamma & \cos \gamma \end{bmatrix} \begin{bmatrix} i_{s\alpha} \\ i_{s\beta} \end{bmatrix} \tag{3}$$

Rotor flux angular “ γ ,” magnetic current “ i_m ” are determined by using the current model corresponding to (4)-(7). The [d-q] is the rotating coordinate system corresponding to the rotor axis.

$$\begin{bmatrix} i_{sd} \\ i_{sq} \end{bmatrix} = \begin{bmatrix} \cos \theta & \sin \theta \\ -\sin \theta & \cos \theta \end{bmatrix} \begin{bmatrix} i_{s\alpha} \\ i_{s\beta} \end{bmatrix} \tag{4}$$

With:

$$\theta = \int \omega_r dt$$

Corresponding to rotor angular

$$\begin{bmatrix} i_{md} \\ i_{mq} \end{bmatrix} = \begin{bmatrix} \frac{1}{T_{R.S}+1} & 0 \\ 0 & \frac{1}{T_{R.S}+1} \end{bmatrix} \begin{bmatrix} i_{sd} \\ i_{sq} \end{bmatrix} \tag{5}$$

$$\begin{bmatrix} i_{m\alpha} \\ i_{m\beta} \end{bmatrix} = \begin{bmatrix} \cos \theta - \sin \theta \\ \sin \theta \cos \theta \end{bmatrix} \begin{bmatrix} i_{md} \\ i_{mq} \end{bmatrix} \tag{6}$$

$$\begin{cases} \gamma = \arctg\left(\frac{i_{m\beta}}{i_{m\alpha}}\right) \\ i_m = \sqrt{(i_{m\alpha}^2 + i_{m\beta}^2)} \end{cases} \tag{7}$$

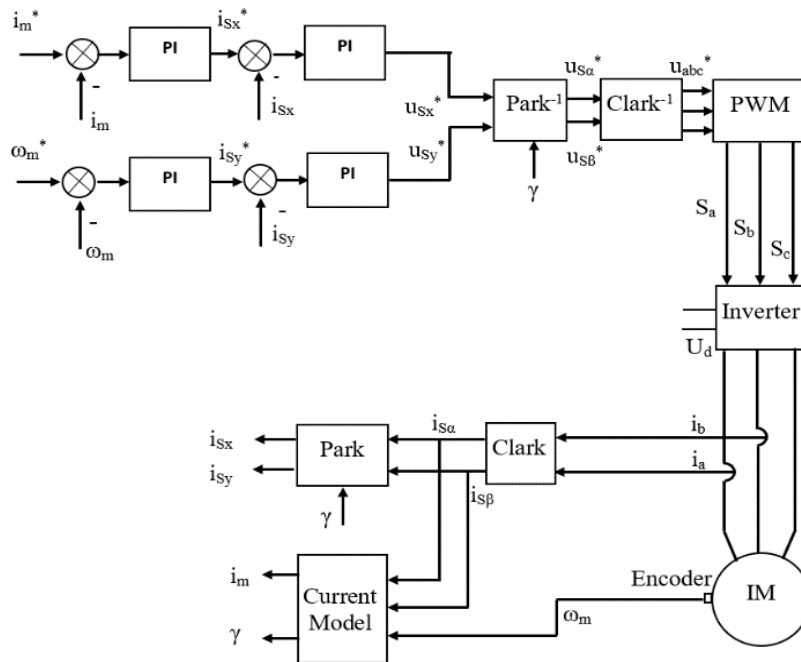


Figure 1. FOC block diagram in IMD

The differences between the reference and the feedback signal in the [x-y] coordinate system will be used to create the command voltage for the switching pulse modulation of the inverter. The inverter will supply the modulation voltage to the three-phase IM corresponding to speed-torque requirements.

2.2. The sensor fault diagnosis technique applied to three-phase IM

A sensor fault diagnosis function, referred to as the fault detection-isolation (FDI) unit, is integrated into the typical FOC method to solve the sensor failures occurring during IMD operation, as shown in Figure 2.

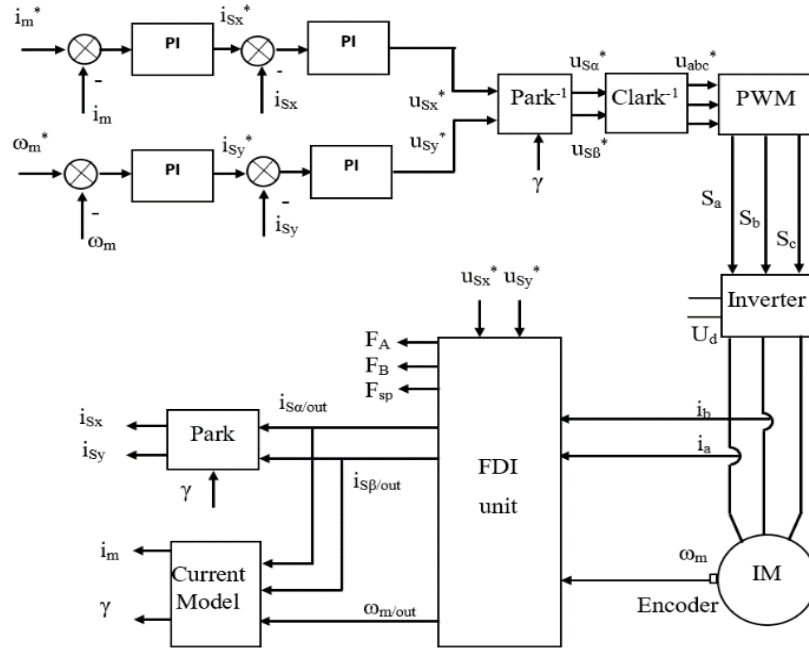


Figure 2. FOC integrated the FDI block diagram in IMD

The FDI unit will receive the feedback signals from sensors, perform a signal quality assessment to decide on the status of sensors, and provide the appropriate output signal to the FOC controller. The diagnosis method will prioritize checking the operating status and quality of the speed feedback signal, as in (8).

$$If(|\omega_m - \omega_{ref}| < Threshold_w) \{F_{sta_sp} = 1; \} Else \{F_{sta_sp} = 0; \} \tag{8}$$

Where: ω_{ref} : the reference speed

F_{sta_sp} : the indicator corresponding stable speed condition

“Threshold_w” is the maximum difference between the measured and reference speed.

Indicator “ F_{sta_sp} ” is delayed for a period of 3τ to ensure that the motor is operating at a steady state.

$$If(F_{sta_sp} = 1) \{Delay[3\tau]: F_{sta_sp}^* = 1; \} \tag{9}$$

Where:

$$\tau = \frac{L_S}{R_S}$$

The current fault diagnosis method will be performed when “ F_{sta_sp} ” and “ $F_{sta_sp}^*$ ” are at high levels (value of 1). The current for each phase will have the form of a sinusoidal function as follows:

$$i_i = I_m \sin(\omega_e t + \phi_i) \tag{10}$$

Where: I_m : amplitude of the phase current

ϕ_i : phase angle of the phase current corresponding to $0^\circ, 120^\circ, -120^\circ$

ω_e : electrical angular frequency

Multiply (10) with the angular frequency and do the integration in the time domain, and we can receive the following function:

$$\omega_e \int i_i = -\omega_e \frac{I_m}{\omega_e} \cos(\omega_e t + \phi_i) = -I_m \cos(\omega_e t + \phi_i) \tag{11}$$

The square root of the sum of squares (10) and (11) gives a constant value in the steady-state operation conditions, as shown in (12):

$$I_m = I_m \sqrt{\sin^2(\omega_e t + \phi_i) + \cos^2(\omega_e t + \phi_i)} \tag{12}$$

By combining the phase current signal and its integral signal according to the trigonometric algorithm (11), we can determine the state of the current signal in steady-state conditions.

We can use the appropriate method to generate an estimated current space vector from voltage signals, measured speed, and machine parameters [26]-[28]. The amplitude of the estimated current space vector can be used for the comparison algorithm to display the fault indicators of the current sensor, as in (13), (14):

$$Index_{cur_i} = |(i_i^2 + (\omega_e \int i_i)^2) - I_m^{est}| \tag{13}$$

$$If(F_{sta_sp} = 1) \&\& (F_{sta_sp}^* = 1) \&\& (Index_{cur_i} > Threshold_I) \{F_i = 1;\} \tag{14}$$

Where: I_m^{est} : the amplitude of the estimated current space vector

F_i : the fault indicator corresponding to a or b phase current

“Threshold_I”: a maximum amplitude deviation of the phase current and estimated current in the normal condition

Using the appropriate method, such as RFMRAS, CB MRAS, Sliding mode [21]-[25], we can generate an estimated rotor speed from voltage signals, measured stator current, and machine parameters. If “ F_{sta_sp} ” is at a low level (value of zero), a comparison algorithm between measured and estimated speed will be performed to identify the speed sensor fault accurately, as in (15), (16):

$$Index_w = |\omega_m - \omega_{est}| \tag{15}$$

$$If(F_{sta_sp} = 0) \&\& (Index_w > Threshold_w) \{F_{sp} = 1;\} \tag{16}$$

After the diagnosis algorithms are performed, the FDI unit will provide the appropriate output signals to the FOC loop. The fault indication status and corresponding output signals are shown in Table 1. This paper uses the sliding mode observer referred to [23] for estimating the rotor speed and the Luenberger observer referred to [28] for virtual current estimation.

Table 1. Judgment principle of FDI unit

Fault indicator	Sensor status	Output
$F_{sp}=0, F_A=0, F_B=0$	Healthy	$\omega_m, i_{s\alpha}, i_{s\beta}$
$F_{sp}=1, F_A=0, F_B=0$	Speed sensor fault	$\omega_{est}, i_{s\alpha}, i_{s\beta}$
$F_{sp}=0, F_A=1, F_B=0$	A-phase current sensor fault	$\omega_m, i_{s\alpha_est}, i_{s\beta_est}$
$F_{sp}=0, F_A=0, F_B=1$	B-phase current sensor fault	$\omega_m, i_{s\alpha_est}, i_{s\beta_est}$

3. RESULTS AND DISCUSSION

In this simulation section, three studies corresponding to each sensor malfunction will be performed to evaluate the effectiveness of the proposed diagnostic method. Parameters of the three-phase motors used in the simulations are listed in Table 2.

Table 2. The IMD parameter

Description	Value
Rated Torque: T_n	14.8 Nm
Rated Speed: ω_n	1420 rpm
Rated current: I_n	4.85 A
Stator, Rotor Resistance: R_s, R_r	3.179/2.118 Ω
Magnetizing Inductance: L_m	0.192 H
Stator, Rotor Inductance: L_s, L_r	0.209/0.209 H
Number of pole pairs: p	2

The induction motor is accelerated from zero to 250 rpm in 0.2 s and maintained to 1.0 s, then the reference speed is increased to 750 rpm as the step function, and the motor is kept operating at this speed, as shown in Figure 3(a). Despite the sudden change in the reference speed, the fault diagnosis function of the FDI unit still works correctly, without any sensor fault recording being warned in the period from zero to 1.5 s. The total speed sensor malfunction occurs at 1.5s, and the value of measured rotor speed change from 750 rpm to zero instantaneously. The diagnosis algorithm based on (8), (15), and (16) in the FDI unit immediately works to identify the failed sensor. In this case, because the feedback speed corresponds to ω_m in (15) and affects the estimated current in (13); therefore, all three indexes increase highly, as in Figure 3(b). However, the diagnosis algorithm correctly identified the speed sensor fault by combining indexes, the F_{stb-sp} , and F_{stb-sp}^* indicators, as shown in Figure 3(c). Figure 3(d) presents the outputs of the FDI unit corresponding to Table 1.

In case 2, the current sensor faults are simulated corresponding to the A-phase current. The total current sensor fault occurs at 1.5s, as shown in Figure 4(a). The diagnosis algorithms based on (13) and (14) are immediately implemented to determine the faulty current sensor. As a result, the index corresponding to the false current phase will increase sharply, as shown in Figure 4(b). Figure 4(c) illustrates the correct diagnosis corresponding to the A-phase current through the fault indication flag. Figure 4(d) presents the outputs of the FDI unit corresponding to Table 1 and the stable operation of IMD.

Similar to the above case, the current sensor faults are simulated corresponding to the B-phase current in case 3. The current failure occurs at 1.5 s, as shown in Figure 5(a). Figure 5(b) indicates that the index corresponding to the B-phase current increases sharply at the time of the occurring fault. The fault indication flag of B-phase current changes from low to high level immediately, as in Figure 5(c). The outputs of the FDI unit and the stable operation of IMD are demonstrated in Figure 5(d).

Through the above three simulation results, the proposed method has accurately detected, located, and isolated each sensor fault, providing appropriate control signals to the FOC loop to maintain the stable operation of IMD even under sensor failure conditions.

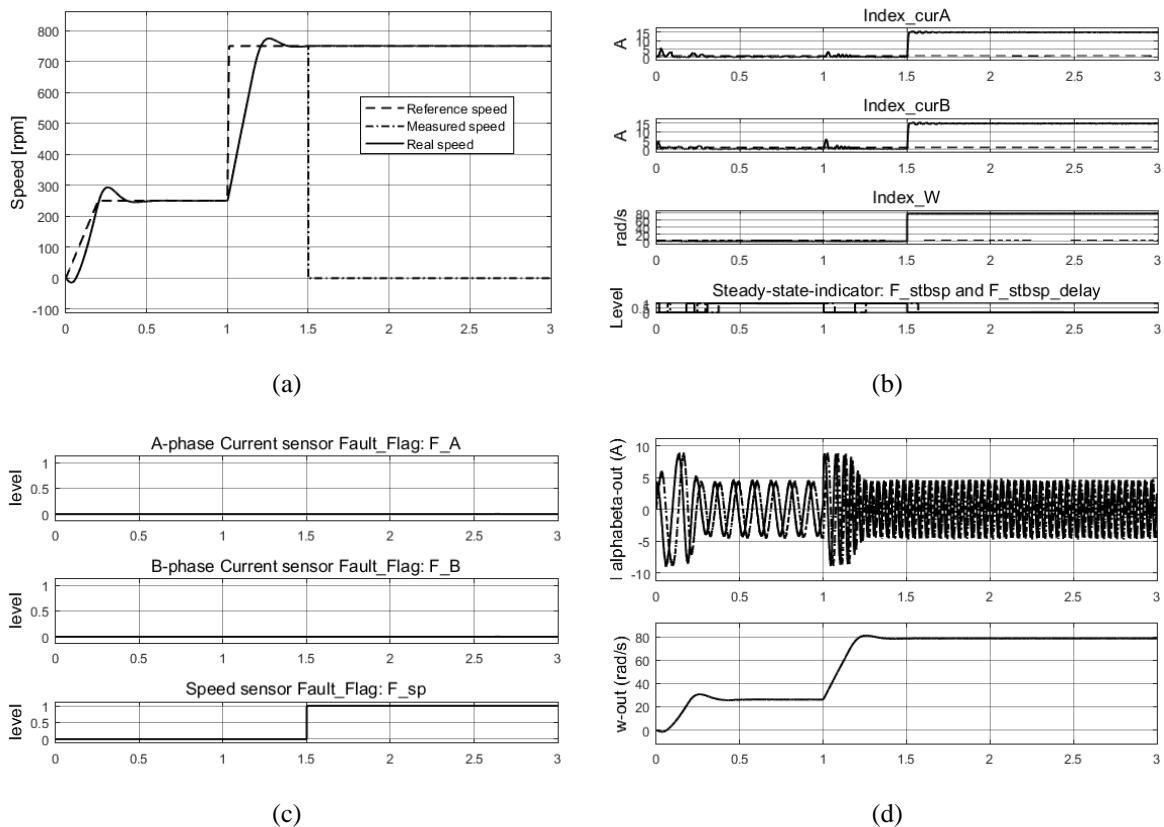


Figure 3. Speed sensor fault diagnosis: (a) rotor speeds, (b) indexes and steady-state indicators, (c) sensor indication flags, and (d) outputs of FDI unit

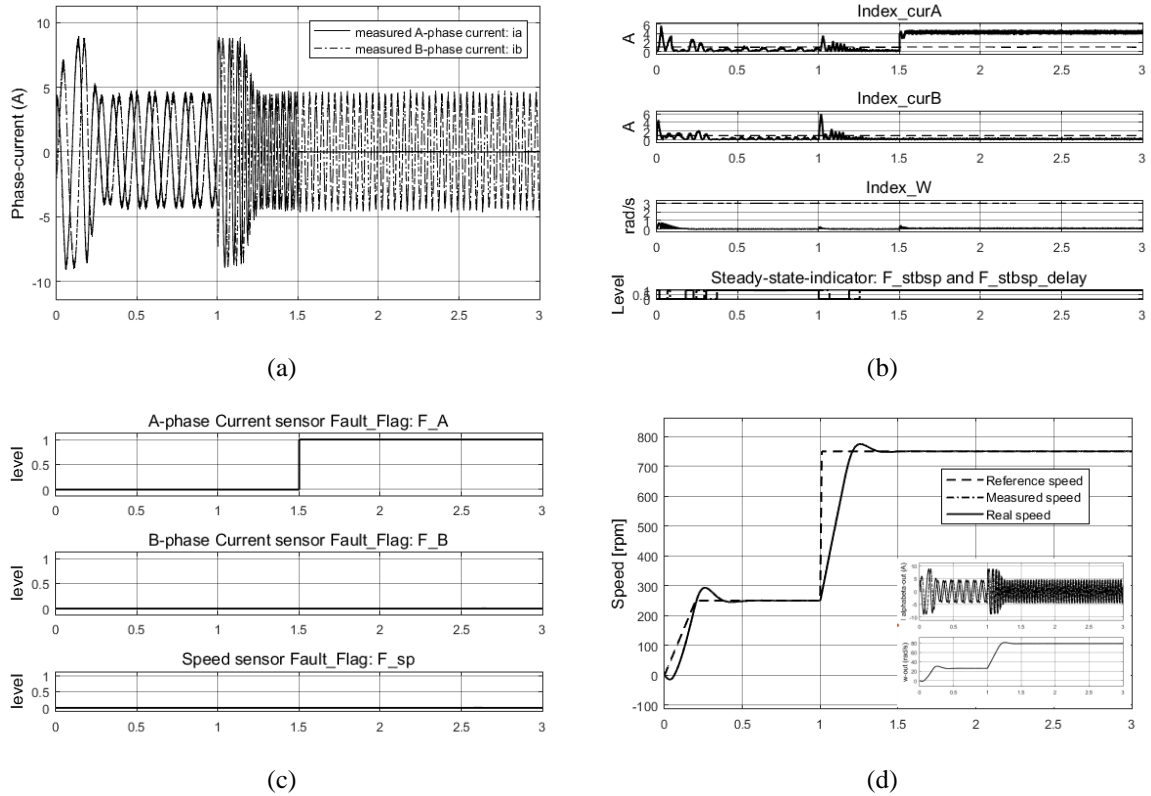


Figure 4. A-phase current sensor fault diagnosis: (a) rotor speeds, (b) indexes and steady-state indicators, (c) sensor indication flags, and (d) outputs of FDI unit

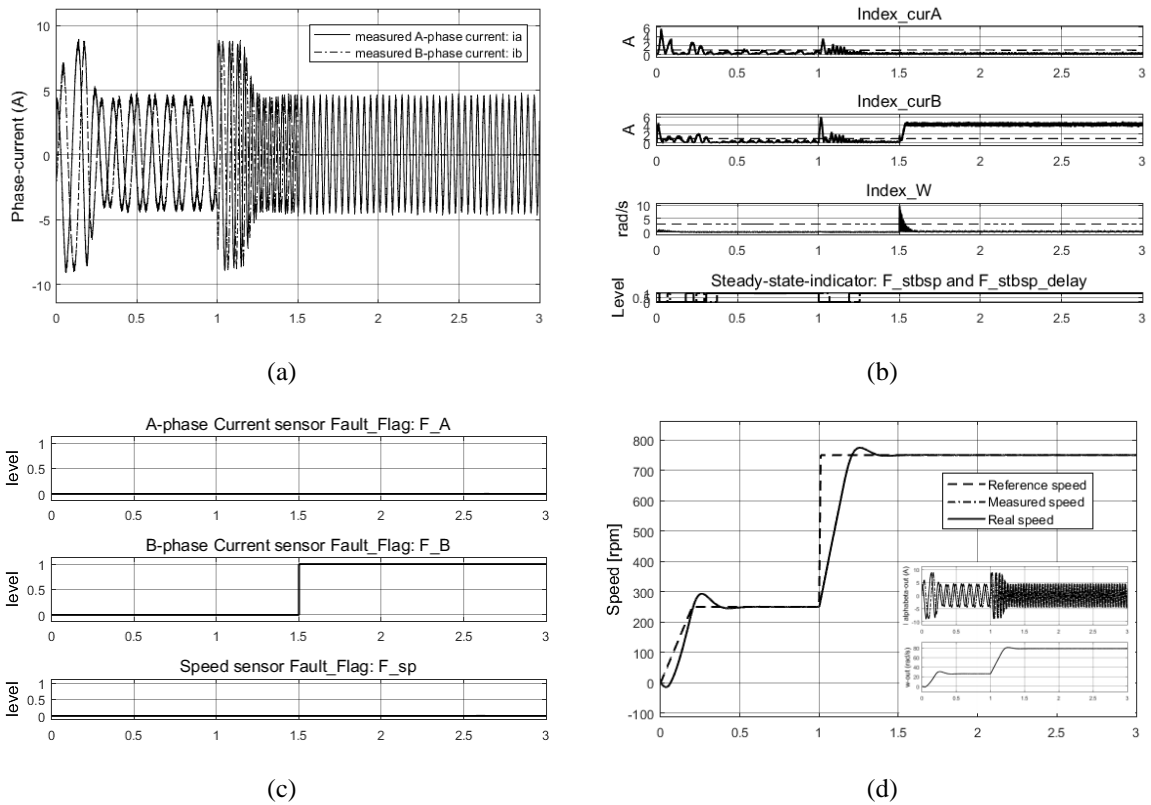


Figure 5. B-phase current sensor fault diagnosis: (a) rotor speeds, (b) indexes and steady-state indicators, (c) sensor indication flags, and (d) outputs of FDI unit

4. CONCLUSION

The paper presents a diagnosis strategy integrated into the FDI unit for speed and current sensor faults of an IMD that operates with two current sensors and a speed encoder. Speed sensor failure is diagnosed based on a measured and estimated rotor speed comparison algorithm. An amplitude value based on the combination of the integral signal and the current signal of each phase is compared to the estimated current for detecting a faulty current sensor. The proposed method accurately diagnoses sensor failures and is not confused with normal operating situations, such as a change in the reference speed of the step function. After evaluating the quality of the feedback signals, the FDI unit will provide appropriate control signals to the FOC-controller to maintain the stable and reliable operation of the IMD. The feasibility of the proposed diagnosis strategy has been verified through simulation results in the fault cases of three sensors.

ACKNOWLEDGEMENTS

This research is funded by Saigon University, Vietnam, 2022, under grant number CSB2022-10.





REFERENCES

- [1] T. F. Chan and K. Shi, *Applied Intelligent Control of Induction Motor Drives*. US: IEEE Press, 2011.
- [2] A. M. Trzynadlowski, *Control of induction motors*. US: Academic Press, 2001.
- [3] AN2388 Application note, "Sensor field oriented control (FOC) of three-phase AC induction motors using ST10F276," *ReVision*, pp. 1–54, 2006.
- [4] W. Li, Z. Xu, and Y. Zhang, "Induction motor control system based on FOC algorithm," in *2019 IEEE 8th Joint International Information Technology and Artificial Intelligence Conference (ITAIC)*, May 2019, pp. 1544–1548, doi: 10.1109/ITAIC.2019.8785597.
- [5] D. L. M. -Nzongo, T. Jin, G. Ekemb, and L. Bitjoka, "Decoupling network of field-oriented control in variable-frequency drives," *IEEE Transactions on Industrial Electronics*, vol. 64, no. 7, pp. 5746–5750, Jul. 2017, doi: 10.1109/TIE.2017.2674614.
- [6] B. Tabbache, M. E. H. Benbouzid, A. Kheloui, and J.-M. Bourgeot, "Virtual-sensor-based maximum-likelihood voting approach for fault-tolerant control of electric vehicle powertrains," *IEEE Transactions on Vehicular Technology*, vol. 62, no. 3, pp. 1075–1083, Mar. 2013, doi: 10.1109/TVT.2012.2230200.
- [7] C. D. Tran, P. Palacky, M. Kuchar, P. Brandstetter, and B. H. Dinh, "Current and speed sensor fault diagnosis method applied to induction motor drive," *IEEE Access*, vol. 9, pp. 38660–38672, 2021, doi: 10.1109/ACCESS.2021.3064016.
- [8] A. A. Amin and K. M. Hasan, "A review of fault tolerant control systems: advancements and applications," *Measurement*, vol. 143, pp. 58–68, Sep. 2019, doi: 10.1016/j.measurement.2019.04.083.
- [9] D. Diallo, M. E. H. Benbouzid, and M. A. Masrur, "Special section on condition monitoring and fault accommodation in electric and hybrid propulsion systems," *IEEE Transactions on Vehicular Technology*, vol. 62, no. 3, pp. 962–964, Mar. 2013, doi: 10.1109/TVT.2013.2245731.
- [10] A. Gouichiche, A. Safa, A. Chibani, and M. Tadjine, "Global fault-tolerant control approach for vector control of an induction motor," *International Transactions on Electrical Energy Systems*, vol. 30, no. 8, pp. 1–17, Aug. 2020, doi: 10.1002/2050-7038.12440.
- [11] A. Raisemche, M. Boukhnifer, C. Larouci, and D. Diallo, "Two active fault-tolerant control schemes of induction-motor drive in EV or HEV," *IEEE Transactions on Vehicular Technology*, vol. 63, no. 1, pp. 19–29, Jan. 2014, doi: 10.1109/TVT.2013.2272182.
- [12] Y. Azzoug, A. Menacer, R. Pusca, R. Romary, T. Ameid, and A. Ammar, "Fault tolerant control for speed sensor failure in induction motor drive based on direct torque control and adaptive stator flux observer," in *2018 International Conference on Applied and Theoretical Electricity (ICATE)*, Oct. 2018, pp. 1–6, doi: 10.1109/ICATE.2018.8551478.
- [13] K. Klimkowski and M. Dybkowski, "A comparative analysis of the chosen speed sensor faults detectors for induction motor drives," in *2015 International Conference on Electrical Drives and Power Electronics (EDPE)*, Sep. 2015, pp. 333–338, doi: 10.1109/EDPE.2015.7325316.
- [14] Y. Yu, Y. Zhao, B. Wang, X. Huang, and D. Xu, "Current sensor fault diagnosis and tolerant control for VSI-based induction motor drives," *IEEE Transactions on Power Electronics*, vol. 33, no. 5, pp. 4238–4248, May 2018, doi: 10.1109/TPEL.2017.2713482.
- [15] L. Baghli, P. Poure, and A. Rezzoug, "Sensor fault detection for fault tolerant vector controlled induction machine," in *2005 European Conference on Power Electronics and Applications*, 2005, pp. 1–10, doi: 10.1109/EPE.2005.219346.
- [16] M. E. Romero, M. M. Seron, and J. A. D. Doná, "Sensor fault-tolerant vector control of induction motors," *IET Control Theory & Applications*, vol. 4, no. 9, pp. 1707–1724, Sep. 2010, doi: 10.1049/iet-cta.2009.0464.
- [17] T. A. Najafabadi, F. R. Salmasi, and P. J. -Maralani, "Detection and isolation of speed, DC-link voltage, and current-sensor faults based on an adaptive observer in induction-motor drives," *IEEE Transactions on Industrial Electronics*, vol. 58, no. 5, pp. 1662–1672, May 2011, doi: 10.1109/TIE.2010.2055775.
- [18] C. Chakraborty and V. Verma, "Speed and current sensor fault detection and isolation technique for induction motor drive using axes transformation," *IEEE Transactions on Industrial Electronics*, vol. 62, no. 3, pp. 1943–1954, Mar. 2015, doi: 10.1109/TIE.2014.2345337.
- [19] M. Manohar and S. Das, "Current sensor fault-tolerant control for direct torque control of induction motor drive using flux-linkage observer," *IEEE Transactions on Industrial Informatics*, vol. 13, no. 6, pp. 2824–2833, Dec. 2017, doi: 10.1109/TII.2017.2714675.
- [20] F. R. Salmasi, "A self-healing induction motor drive with model free sensor tampering and sensor fault detection, isolation, and compensation," *IEEE Transactions on Industrial Electronics*, vol. 64, no. 8, pp. 6105–6115, Aug. 2017, doi: 10.1109/TIE.2017.2682035.
- [21] M. Kuchar, P. Brandstetter, and M. Kaduch, "Sensorless induction motor drive with neural network," in *2004 IEEE 35th Annual Power Electronics Specialists Conference (IEEE Cat. No.04CH37551)*, 2004, pp. 3301–3305, doi: 10.1109/PESC.2004.1355058.





- [22] P. Brandstetter, "Sensorless control of induction motor using modified MRAS," *International Review of Electrical Engineering*, vol. 7, no. 3, pp. 4404–4411, 2012.
- [23] C. S. T. Dong, C. D. Tran, S. D. Ho, P. Brandstetter, and M. Kuchar, "Robust sliding mode observer application in vector control of induction motor," in *2018 ELEKTRO*, May 2018, pp. 1–5, doi: 10.1109/ELEKTRO.2018.8398291.
- [24] P. Brandstetter, M. Dobrovsky, M. Kuchar, C. S. T. Dong, and H. H. Vo, "Application of BEMF-MRAS with Kalman filter in sensorless control of induction motor drive," *Electrical Engineering*, vol. 99, no. 4, pp. 1151–1160, Dec. 2017, doi: 10.1007/s00202-017-0613-4.
- [25] T. O. -Kowalska and M. Dybkowski, "Stator-current-based MRAS estimator for a wide range speed-sensorless induction-motor drive," *IEEE Transactions on Industrial Electronics*, vol. 57, no. 4, pp. 1296–1308, Apr. 2010, doi: 10.1109/TIE.2009.2031134.
- [26] S. D. Ho, P. Brandstetter, P. Palacky, M. Kuchar, B. H. Dinh, and C. D. Tran, "Current sensorless method based on field-oriented control in induction motor drive," *Journal of Electrical Systems*, vol. 17, no. 1, pp. 62–76, 2021.
- [27] C. D. Tran, T. X. Nguyen, and P. D. Nguyen, "A field-oriented control (FOC) method using the virtual currents for the induction motor drive," *International Journal of Power Electronics and Drive Systems (IJPEDS)*, vol. 12, no. 4, pp. 2095–2102, Dec. 2021, doi: 10.11591/ijpeds.v12.i4.pp2095-2102.
- [28] Y. Azzoug, R. Pusca, M. Sahraoui, A. Ammar, R. Romary, and A. J. M. Cardoso, "A single observer for currents estimation in sensor's fault-tolerant control of induction motor drives," in *2019 International Conference on Applied Automation and Industrial Diagnostics (ICAAID)*, Sep. 2019, pp. 1–6, doi: 10.1109/ICAAID.2019.8934969.

BIOGRAPHIES OF AUTHORS







Tien Xuan Nguyen     was born in 1965, received a Bachelor of Physics-Specialization in Nuclear Electronics from Dalat University in 1988, and a Master's Degree in Mechatronics Engineering from the University City of Technology, Ho Chi Minh City in 2014. Currently, he is a lecturer in the Department of Electrical-Electronics, Faculty of Electronics and Telecommunications of Saigon University. The field of research now controls robots, mechatronics systems and applications, and machine control methods. He can be contacted at email: tien.nx@sgu.edu.vn.



Minh Chau Huu Nguyen     is a lecturer in Faculty of Electrical-Electronics Engineering at Vietnam Aviation Academy. He graduated from the Military Technical Academy, Vietnam, and received his ME degree in Automation Engineering in 2012. He is researching at the Faculty of Electrical Engineering & Computer Science, VSB – Technical University of Ostrava, Czech Republic. His research interests include automatic control systems, intelligent control systems, electrical machines, apparatus, and drives. He can be contacted at email: minhnhc@vaa.edu.vn.



Cuong Dinh Tran     is a lecturer in Faculty of Electrical-Electronic Engineering at Ton Duc Thang University. He received his BE, and ME degrees from Ho Chi Minh City University of Technology, Vietnam, and his Ph.D. from VSB-Technical University of Ostrava, the Czech Republic, in 2005, 2008, and 2020. His research interests include the field of modern control methods and intelligent algorithms in motor drives. He can be contacted at email: trandinhcuong@tdtu.edu.vn.